6-14-2005

Predicting plot basal area and tree density in mixed-conifer forest from lidar and Advanced Land Imager (ALI) data

Andrew T. Hudak
Rocky Mountain Research Station, ahudak@fs.fed.us

Jeffrey S. Evans
Rocky Mountain Research Station

Michael J. Falkowski
University of Idaho, Falk4587@uidaho.edu

Nicholas L. Crookston
Rocky Mountain Research Station, ncrookston@fs.fed.us

Paul E. Gessler
University of Idaho, paulg@uidaho.edu

See next page for additional authors

Predicting plot basal area and tree density in mixed-conifer forest from lidar and Advanced Land Imager (ALI) data

Andrew T. Hudak[1], Jeffrey S. Evans[1], Michael J. Falkowski[2], Nicholas L. Crookston[1], Paul E. Gessler[2], Penelope Morgan[2], and Alistair M.S. Smith[2]

[1]USDA Forest Service, Rocky Mountain Research Station, 1221 South Main Street, Moscow, ID 83843; email: ahudak@fs.fed.us

[2]University of Idaho, Department of Forest Resources, Moscow, ID 83844-1133

ABSTRACT

Multispectral satellite imagery are appealing for their relatively low cost, and have demonstrated utility at the landscape level, but are typically limited at the stand level by coarse resolution and insensitivity to variation in vertical canopy structure. In contrast, lidar data are less affected by these difficulties, and provide high structural detail, but are less available due to their comparatively high cost. Two forest structure attributes measured at the plot level, basal area and trees per hectare, were predicted using stepwise multiple regression on 40 predictor variables derived from discrete-return lidar data (2 m post spacing), Advanced Land Imager (ALI) multispectral (30 m resolution) and panchromatic (10 m resolution) images, and geographic X,Y,Z location. Square root and natural logarithm transforms were applied to normalize the positively skewed response variables. Stepwise variable selection used the AIC statistic to guard against overfitting. Models predicting the transformed variables explained 80-93% of variance, based on 20-22 predictor variables. Lidar-derived variables had the most explanatory power; especially height and intensity variables for predicting plot basal area, and cover and intensity variables for predicting tree density. The ALI variables were less useful for predicting these attributes of forest structure, but could prove more helpful for predicting attributes of forest composition.

Keywords: data integration, forest management, northern Idaho, stepwise regression

1 INTRODUCTION

Image data are sensitive to structural variation between forest stands in the horizontal plane but are relatively insensitive to canopy height variation in the vertical plane. On the other hand, light detection and ranging (lidar) data are actual measurements of canopy height relative to an estimated ground height, providing detailed vertical structure information. Recognizing that image and lidar data provide fundamentally different views of forest structure, and that no single remote sensor can provide all of the information useful and relevant to forest managers, the integration of image and lidar data for the purpose of predicting, mapping, managing and monitoring forest structure attributes is a logical and worthwhile goal [1].

Landsat has become the standard satellite imagery relied upon by many forest ecologists and managers [2]. Sensor age and degradation make the future availability and quality of Landsat 5 Thematic Mapper (TM) data increasingly suspect, while Landsat 7 Enhanced Thematic Mapper Plus (ETM+) has operated with reduced utility since a scan line corrector anomoly began on 31 May 2003 (http://landsat.usgs.gov/programnews.html). Considering the potential imminent failure of both Landsat 5 and 7, the only Landsat sensors still operating, there is justifiable concern for maintaining Landsat data coverage. The Advanced Land Imager (ALI) satellite sensor was designed in part to provide future data continuity with the Landsat record (http://eo1.usgs.gov/ali.php). Although the ALI swath width (37 km) is more restricted than that of Landsat (185 km), and ALI acquisitions must be scheduled in advance, the ALI sensor is pointable. The ALI measures solar irradiance in 9 multispectral bands between 0.433 and and 2.35 µm, providing 3 more multispectral bands than Landsat TM or ETM+. The spatial resolution of the panchromatic (PAN) band is 10 m, compared to the 15 m resolution of the ETM+ panchromatic

Presented at the 26th Canadian Symposium on Remote Sensing in Wolfville, Nova Scotia, June 14-16, 2005

band. Furthermore, ALI data are 16-bit rather than 8-bit, offering greater dynamic range. A comparative study [3] found no disadvantages of the ALI sensor relative to the TM or ETM+ sensors, and recommended the ALI sensor for a potential Landsat 8 payload.

Numerous studies have demonstrated the utility of lidar for characterizing various attributes of forest canopy structure from discrete-return lidar data [4],[5],[6]. Enthusiasm for lidar-based forest inventory is driving expansion of the commercial lidar industry [7]. As the costs of managing forested landscapes increase in a competitive environment, commercial timber and paper companies are increasingly turning to lidar for potentially more accurate and efficient inventory and assessment of their forest resources.

Many have recognized the potential advantages of remote sensing data integration [1],[7],[8]. One study compared the utility of several remotely sensed datasets for forest inventory, monitoring and mapping in high-biomass forests of western Oregon [8]. Another fused lidar and multispectral image data to improve estimates of individual tree height [9]. Rather than evaluate many remote sensing products, this analysis used single acquisitions of ALI satellite imagery and commercial discrete-return lidar data, much like a future commercial forester with limited time and resources might. Also, rather than identify individual trees, this analysis focused on two stand-level attributes: plot basal area and tree density. Finally, rather than "fuse" remotely sensed data layers, or test a variety of data integration methods, this analysis focused on probably the simplest and most widely applied data "integration" method: stepwise multiple regression. In that sense, the "data integration" conducted via stepwise multiple regression is purely statistical, but provides the most accessible and objective means of comparing and selecting remotely sensed data layers for predicting attributes of interest to operational forest managers.

2 METHODS

2.1 Study Area

The Moscow Mountain and St. Joe Woodlands study areas together comprise >88,000 ha in north-central Idaho. Both areas are topographically diverse, with the higher elevations and steeper slopes occurring in the St. Joe Woodlands. Windblown volcanic ash from the Cascade Mountains acts as an important soil component in both areas. Conifer species range along a moisture gradient from *Pinus ponderosa* and *Pseudotsuga menziesii* at the drier end, more commonly found on southern aspects in the Moscow Mountain area, to *Thuja plicata* and *Tsuga heterophylla* at the wetter end, more commonly found on northern aspects especially in the St. Joe Woodlands. Other important species include *Abies grandis*, *Abies lasiocarpa*, *Larix occidentalis*, *Picea engelmannii*, *Pinus contorta*, and *Pinus monticola*. These forests are actively managed, with most having been logged at least once, and very little never logged. Industry partners Potlatch, Inc. and Bennett Lumber Products, Inc. are the principal land owners of Moscow Mountain and the St. Joe Woodlands, respectively.

2.2 Field Sampling

Field sites were selected in each study area using a two-stage stratified design, with the first stage based on 3 elevation and 3 solor insolation classes generated from a 30 m USGS DEM, then crossed to produce 9 strata. Solar insolation, which incorporates into a single variable the important biophysical drivers of slope and aspect, was calculated using Solar Analyst [10]. The second stage assiged 9 leaf area index (LAI) classes into each of the 9 strata, where LAI was indicated by a mid-infrared corrected Normalized Difference Vegetation Index (NDVIc) [11],[12] calculated from August 2002 Landsat ETM+ multispectral imagery. Landsat pixels spanning the LAI gradient within each strata were then systematically selected, which resulted in 81 target plots distributed across each study area in a spatially random pattern. These target plots were loaded as waypoints into a Global Positioning System (GPS). Once navigated to in the field, plot centers were geolocated using the GPS by logging a minimum of 150 points; these were later differentially corrected upon returning from the field and then averaged to get a final 3-D point position. The sizes of the fixed-radius plots were 0.04 ha (1/10 acre) at Moscow Mountain and 0.08 ha (1/5 acre) at the St. Joe Woodlands. Within each plot, the diameter at breast height (dbh) of all trees >12.7 cm (5 in.) was measured. Eleven of the plots on Moscow Mountain did not have trees >12.7 cm dbh but were included in this analysis. In addition, two supplementary plots were sampled to characterize old-growth stands (one in each study area), which because of their rarity were not selected through the stratification process, but were considered important for sampling the upper end of the vegetation biomass gradient, and nonetheless interesting to characterize

from a research or management perspective. Although the two old-growth stands were necessarily subjectively selected, the plot centers within each stand were randomly located.

2.3 Image Processing

ALI data were acquired 1 October 2004 for Moscow Mountain from an overhead pass, and 3 October 2004 for the St. Joe Woodlands from an east path looking west. The Level 1R product was purchased, which was radiometrically but not geometrically corrected (http://eo1.usgs.gov/userGuide/ali_process.html). Both the single-band panchromatic and nine-band multispectral images were delivered as four separate image strips, which were mosaicked in ENVI following online instructions (http://eo1.usgs.gov/faq.php?id=31). The seamless mosaicked images were then coregistered in Imagine to an orthorectified Landsat ETM+ panchromatic image base (26 Aug 1999, Path 42 / Row 27), using image tie-points (ITPs) automatically generated using an automated, area-based correlation algorithm coded in IDL [13]. For Moscow Mountain, cumulative root mean square (RMS) errors were 1.9 m (N = 202 ITPs) for the panchromatic band and 8.5 m (N = 78 ITPs) for the multispectral band; for the St. Joe Woodlands, cumulative RMS errors were 5.0 m (N = 82 ITPs) for the panchromatic band and 3.6 m (N = 106 ITPs) for the multispectral band. The georectified images were then converted to ArcInfo GRIDs. Textural images were generated from the panchromatic images using the FOCALSTD function with a 3x3 filter window. Simple Ratio (SR = band 5 / band 4), Green Red Vegetation Index (GRVI = (band 3 – band 4) / (band 3 + band 4)), and Normalized Difference Vegetation Index (NDVI = (band 5 – band 4) / (band 5 + band 4)) were generated from the multispectral images. The pixel value at the center point of each plot was extracted from the ten raw ALI bands and four derived indices.

2.4 Lidar Processing

Lidar data were acquired in July, August or September 2003 for Moscow Mountain (32,708 ha) and the St. Joe Woodlands (55,684 ha). Raw X,Y,Z positions were delivered as ASCII files corresponding to each flight line. To identify ground returns, a curvature thresholding approach termed "virtual deforestation" (VDF), which iteratively identifies and removes vegetation returns until only ground returns remain, was used [14]. This VDF technique was coded in ArcInfo Macro Language (AML) and improved upon by incorporating variable window sizes into the procedure (Evans and Hudak in prep). Subsequent interpolation of these ground returns using bicubic splines produced an accurate bare earth digital elevation model (DEM) at a resolution matching the post spacing of the lidar survey (2 m). The DEM was then simply subtracted from the raw height returns to calculate canopy height for all lidar points sampled. At a cell size of 6 m, ArcInfo GRIDs of canopy height, cover, and intensity were generated across both landscapes. Canopy cover was calculated as the proportion of canopy returns to total (ground + canopy) returns within each 6 m cell. These grids were used to calculate minimum, maximum, mean, standard deviation and sum statistics for canopy height, cover, and intensity within each plot footprint, using the ZONALSTATS function in GRID. In addition within each plot footprint, the minimum, maximum, mean, 25^{th}, 50^{th} (median), 75^{th} percentiles, and interquantile range of canopy height were calculated from the point canopy height data >6 cm (essentially excluding from the calculation the ground returns within the vertical estimation error of ground height in the DEM). Percent canopy cover was also calculated from the point data within each plot footprint, again as the ratio of canopy to total returns.

2.5 Statistical Analysis

The 40 predictor variables (x's) used in this analysis consisted of 12 lidar-derived canopy height variables, 6 lidar-derived cover variables, 5 lidar intensity variables, 14 ALI-derived variables, and geographic X,Y,Z location of the plot centers. The two response variables (y's) of interest were plot basal area (Plot_BA; m^2/ha) and tree density (Plot_TPH; trees/ha). Stepwise regression was performed using the "step" function of the "stats" package in R. Variable selection was based on the Akaike Information Criterion (AIC) statistic [15] to guard against overfitting.

3 RESULTS

Because both response variables were positively skewed, square root (SQRT) and natural logarithm (LN) transforms were applied. The SQRT transform did a better job of normalizing the distributions than LN, which overcorrected and caused some negative skew (Figure 1).

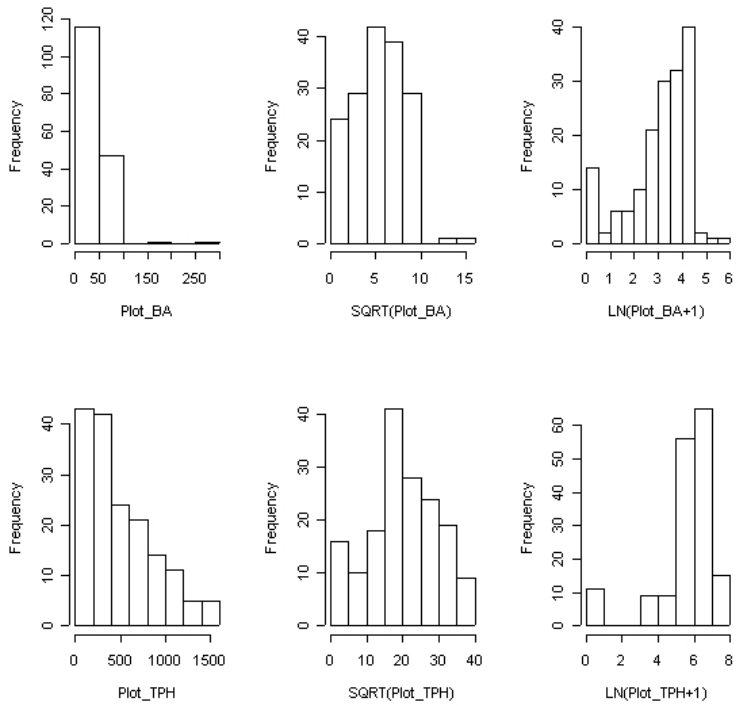

Figure 1. Histograms of untransformed, square root (SQRT) transformed, and natural logarithm (LN) transformed plot basal area (Plot_BA; m^2/ha) and tree density (Plot_TPH; trees/ha) observed on all plots (N = 165). The two rightmost columns in the top row of Plot_BA histograms are the two supplementary old-growth plots.

Model fits were better for plot basal area than for tree density. The SQRT and LN transformed response variables produced much better model fits (higher R^2 and Adjusted R^2; lower SE and AIC) than the untransformed response variables, with the LN transform producing the best fits, for both plot basal area and tree density. Because the SQRT and LN transforms so markedly improved the models, only these were broken down into specific predictor variable groupings (Table 1). Models based on just the geographic variables proved the worst predictors; models based on just the lidar variables were the best predictors; models based on just the ALI predictors were intermediate predictors. ALI variables were better predictors of tree density than plot basal area. Lidar height variables were the best predictors of plot basal area, followed by the intensity variables, while lidar-derived cover variables were the best predictors of tree density, again followed by the intensity variables. Models using lidar and ALI predictor variables were not much improved over models using just lidar variables.

The SQRT and LN transforms reduced heteroskedasticity in the response variables, as indicated by the more random distribution of residuals (Figure 2). In the case of tree density, the LN tranformation overly skewed the predictions towards the higher values, producing a gap between the forested (N = 154) and nonforested (N = 11) plots. Predicted values from the SQRT and LN transformed full models were backtranformed, and then the observed values regressed on the predicted values, to quantify the bias introduced by the transformations, as indicated by the slope (b) of the simple linear model with the intercept forced to zero. Compared to the untransformed full model, which is perfectly unbiased (b = 1), the SQRT transform introduced less bias (b = 1.029) than the LN transform (b = 0.956) for predicting plot basal area. For tree density, the SQRT transform introduced slightly more bias (b = 1.048) than the LN transform (b = 1.021).

Summary statistics from the full models revealed an underprediction problem at the extremes of the distribution when no transformation was applied (Table 2). The LN tranform full model did the best job of predicting the higher plot basal area and tree density values, the 25th, 50th, and 75th quantile statistics for tree density, and the median and mean for plot basal area. The SQRT transform full model did the best job of predicting the 25th and 75th quantiles for plot basal area.

Table 1. Stepwise regression results for predicting A) plot basal area (Plot_BA; m^2/ha), and B) tree density (Plot_TPH; trees/ha) based on all field plots (N = 165) and up to 40 predictor variables including: geographic X,Y,Z location; Advanced Land Imager raw (10) and derived (4) bands; and lidar canopy height, cover and intensity. All models were statistically significant ($p < 0.05$). Standard error (SE) and AIC statistics should only be directly compared between the solid lines.

Variable Groupings	Available	Selected	SE	R2	Adj. R2	AIC
A) Plot Basal Area (Plot_BA; m2/ha)						
Predict Plot_BA (x's = all)	40	17	15.84	0.7890	0.7646	928.48
Predict SQRT(Plot_BA) (x's = all)	40	20	0.93	0.9051	0.8920	-5.61
XYZ location	3	3	2.63	0.1436	0.1276	323.44
ALI + Lidar	37	18	0.97	0.8936	0.8805	9.34
ALI spectral	14	9	2.09	0.4815	0.4514	252.63
Lidar Ht + CC + Int	23	11	1.08	0.8622	0.8523	37.95
Height (Ht)	12	4	1.25	0.8075	0.8027	79.16
Canopy Cover (CC)	6	3	1.73	0.6308	0.6239	184.60
Intensity (Int)	5	3	1.53	0.7106	0.7052	144.41
Predict LN(Plot_BA+1) (x's = all)	40	22	0.33	0.9422	0.9333	-346.15
XYZ location	3	3	1.17	0.1670	0.1515	56.14
ALI + Lidar	37	20	0.35	0.9390	0.9247	-327.88
ALI spectral	14	8	0.88	0.5445	0.5211	-33.45
Lidar Ht + CC + Int	23	12	0.38	0.9169	0.9104	-306.21
Height (Ht)	12	4	0.56	0.8109	0.8061	-186.47
Canopy Cover (CC)	6	3	0.63	0.7559	0.7514	-146.41
Intensity (Int)	5	3	0.55	0.8150	0.8116	-192.13
B) Tree Density (Plot_TPH; trees/ha)						
Predict Plot_TPH (x's = all)	40	23	210.90	0.7374	0.6946	1788.07
Predict SQRT(Plot_TPH) (x's = all)	40	22	4.35	0.8238	0.7965	506.08
XYZ location	3	3	9.03	0.1382	0.1221	729.99
ALI + Lidar	37	13	4.50	0.7992	0.7819	509.65
ALI spectral	14	5	7.07	0.4786	0.4622	651.07
Lidar Ht + CC + Int	23	12	4.62	0.7870	0.7702	517.37
Height (Ht)	12	4	6.57	0.5464	0.5351	626.08
Canopy Cover (CC)	6	4	5.43	0.6901	0.6824	563.20
Intensity (Int)	5	3	5.25	0.7083	0.7028	551.26
Predict LN(Plot_TPH+1) (x's = all)	40	21	0.58	0.9025	0.8881	-159.24
XYZ location	3	3	1.59	0.1787	0.1634	156.32
ALI + Lidar	37	22	0.59	0.9015	0.8862	-155.58
ALI spectral	14	8	1.11	0.6122	0.5923	42.51
Lidar Ht + CC + Int	23	11	0.61	0.8848	0.8766	-151.85
Height (Ht)	12	5	1.24	0.5062	0.4906	76.38
Canopy Cover (CC)	6	4	0.70	0.8425	0.8385	-114.14
Intensity (Int)	5	3	0.77	0.8051	0.8015	-81.07

Table 2. Summary statistics of observed and predicted A) plot basal area (Plot_BA; m^2/ha), and B) tree density (Plot_TPH; trees/ha), based on all plots (N = 165).

A)	Min.	1st Qu.	Median	Mean	3rd Qu.	Max.
Observed Plot_BA	0.0	12.0	30.2	36.4	55.8	255.4
Predicted Plot_BA						
No Transformation	-15.6	13.8	35.4	36.4	55.2	149.6
SQRT Transform	0.0	12.1	31.4	35.6	54.2	158.4
LN Transform	-0.1	10.8	29.8	35.8	53.3	230.2

B)	Min.	1st Qu.	Median	Mean	3rd Qu.	Max.
Observed Plot_TPH	0.0	197.7	395.4	492.0	679.5	1594.0
Predicted Plot_TPH						
No Transformation	-151.1	265.1	494.8	492.0	739.6	1213.0
SQRT Transform	0.0	218.7	465.9	475.8	703.9	1241.0
LN Transform	-0.1	208.5	438.2	467.8	686.8	1791.0

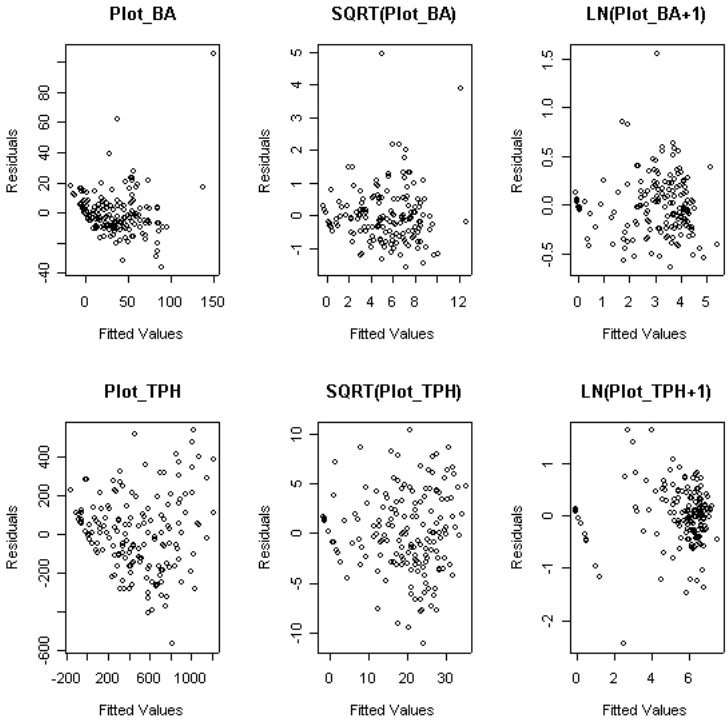

Figure 2. Scatterplots of fitted values vs. residuals from stepwise regression models for predicting untransformed, square root (SQRT) transformed, or natural log (LN) transformed plot basal area (Plot_BA; m^2/ha) and tree density (Plot_TPH; trees/ha).

4 DISCUSSION

Applying SQRT or LN transforms to the response variables improved the performance of the models. Biases introduced by these transforms to the response variables were <5%, or quite minor. Generalized linear models, which require no transformations of the response variables, could also be applied appropriately as an alternative.

Lidar-derived predictor variables explained the most variance in the models, especially for plot basal area. The addition of ALI variables to the models did not improve them much over models based on lidar data alone, possibly due to the inclusion of the intensity values, which were more powerful predictors than expected. Intensity data typically have not been used in vegetation modeling and mapping; their apparent utility needs to be better evaluated and exploited. Value might be added to the ALI imagery by including measures of plot-level pixel variability, as was done with the lidar variables. Other predictor variables could be generated from the lidar canopy returns, such as canopy gap fraction. Solar insolation is an important topographic variable that should be added to the analysis.

Both plot basal area and tree density are purely structural attributes. The lidar canopy height variables were more influential in predicting plot basal area than tree density, while the lidar canopy cover variables were more influential in predicting tree density than plot basal area. This was expected given that stands with larger trees are also taller, while denser stands vary more in the horizontal domain, where cover measures are more sensitive. The ALI imagery, which proved not very helpful in this statistical data integration exercise, should prove more useful for mapping tree species composition or habitat type, because multispectral imagery is more sensitive to this source of variability than the lidar operating at a single wavelength. Moreover, including multispectral image time series in this data integration approach might prove profitable, by capturing phenological variability.

5 CONCLUSION

Simple and straightforward stepwise multiple regression models explained ~90% of variance in two stand-level structure attributes of particular interest to forest managers, using only remotely sensed and geographic predictor

variables. Lidar-derived measures of canopy height, cover, and intensity alone appear capable of explaining this proportion of variance in forest structure attributes. Adding predictor variables derived from multispectral ALI imagery did not provide much additional explanatory power in this analysis of two purely structural attributes, but may be helpful for predicting attributes of forest composition. The logical next step in this application is to refine the statistical data integration models as discussed above and then use the resulting model coefficients to map attributes of forest structure and composition for the benefit of our industry partners and other area forest managers.

ACKNOWLEDGMENTS

This is a product of the Sustainable Forestry component of Agenda 2020, a joint effort of USDA Forest Service Research & Development and the American Forest and Paper Association. Funds were provided by the Rocky Mountain Research Station. Research partners included Potlatch, Inc. and Bennett Lumber Products, Inc. Curtis Kvamme, KC Murdock, Jacob Young, Tessa Jones, Jennifer Clawson, Kasey Prestwich, Bryn Parker, Stephanie Jenkins, and Kris Poncek assisted in the field.

REFERENCES

[1] HUDAK, A.T., LEFSKY, M.A., COHEN, W.B., AND BERTERRETCHE, M. 2002: Integration of lidar and Landsat ETM+ data for estimating and mapping forest canopy height. *Remote Sensing of Environment* 82, pp. 397-416.
[2] COHEN, W.B., AND GOWARD, S.N., 2004: Landsat's role in ecological applications of remote sensing. *BioScience* 54, pp. 535-545.
[3] BRYANT, R.B., MORAN, M.S., MCELROY, S.A., HOLIFIELD, C.D., THOME, K.J., MIURA, T., AND BIGGAR, S.F., 2003: Data continuity of Earth Observing-1 (EO-1) Advanced Land Imager (ALI) and Landsat TM and ETM+. *IEEE Transactions On Geoscience And Remote Sensing* 41, pp. 1204-1214.
[4] NELSON, R., 1984: Determining forest canopy characteristics using airborne laser data. *Remote Sensing of Environment* 15, pp. 201-212.
[5] NILSSON, M., 1996: Estimation of tree heights and stand volume using an airborne Lidar system. *Remote Sensing of Environment* 56, pp. 1-7.
[6] MEANS, J.E., ACKER, S.A., FITT, B.J., RENSLOW, M., EMERSON, L., AND HENDRIX, C.J., 2000: Predicting forest stand characteristics with airborne scanning lidar. *Photogrammetric Engineering and Remote Sensing* 66, pp. 1367-1371.
[7] FLOOD, M., 2001: Laser altimetry: From science to commercial lidar mapping. *Photogrammetric Engineering and Remote Sensing* 67, pp. 1209-1217.
[8] LEFSKY, M.A., COHEN, W.B., AND SPIES, T.A., 2001: An evaluation of alternate remote sensing products for forest inventory, monitoring, and mapping of Douglas-fir forests in western Oregon. *Canadian Journal of Forest Research* 31, pp. 78-87.
[9] POPESCU, S.C., AND WYNNE, R.H., 2004: Seeing the trees in the forest: using lidar and multispectral data fusion with local filtering and variable window size for estimating tree height. *Photogrammetric Engineering and Remote Sensing* 70, pp. 589-604.
[10] HELIOS ENVIRONMENTAL MODELING INSTITUTE (HEMI) LLC, 2000: The Solar Analyst 1.0 User Manual.
[11] NEMANI, R., PIERCE, L., RUNNING, S., AND BAND, L., 1993: Forest ecosystem processes at the watershed scale: sensitivity to remotely-sensed leaf area index estimates. *International Journal of Remote Sensing* 14, pp. 2519–2534.
[12] POCEWICZ, A., GESSLER, P.E., AND ROBINSON, A.P., 2004: The relationship between leaf area index and Landsat spectral response across elevation, solar insolation, and spatial scales, in a northern Idaho forest. *Canadian Journal of Forest Research* 34, pp. 65-480.
[13] KENNEDY, R.E., AND COHEN, W.B., 2003: Automated designation of tie-points for image-to-image coregistration. *International Journal of Remote Sensing* 24, pp. 3467-3490.
[14] HAUGERUD, R.A., AND HARDING, D.J., 2001: Some algorithms for virtual deforestation (VDF) of lidar topographic survey data. *International Archives of Photogrammetry and Remote Sensing* XXXIV, pp. 211–217.
[15] AKAIKE, H., 1973: Information theory and an extension of the maximum likelihood principal. In: Petrov, B.N., and Csaki, F. (eds.): *2nd International Symposium on Information Theory*, pp. 267-281. Academiai Kiado, Budapest.